Incorporation of Relief in Polynomial-Based Geometric Corrections

Vicenç Palà and Xavier Pons

Abstract

This study focuses on the geometrical deformations introduced by relief in images captured by the TM sensor of Landsat satellites and by the HRV sensor of SPOT satellites. Different correction alternatives are presented in order to incorporate altitude data into correction procedures based on first-degree polynomial models. Column and row determinations from the corresponding map coordinates are carried out independently. Three different models for columns and two for rows are proposed. The results have been contrasted with those obtained using classic first- and second-degree polynomial calculations, and with those obtained using an orbital model (for SPOT images). The models presented are easy to implement and provide a level of precision similar to that of the orbital model used, while they are much more efficient in calculation time. In view of the results, the model which integrates altimetric data into a single first-degree polynomial seems of particular interest.

Introduction

Due to the complex characteristics of the Earth-sensor system, images obtained from resource observation satellites suffer from several distortions that make them not directly superimposable on a map. Among those characteristics, we might mention the deformation produced by the conical perspective in which the images are captured, aggravated by Earth curvature and relief, the simultaneous movements of terrestrial rotation and satellite orbit during image capture, and the attitude of the sensor in space, which, whether involuntarily or intentionally, does not always have a view perpendicular to the terrain surface at the center of the image. This last factor is of particular importance in the SPOT satellite, capable of taking images with a lateral inclination angle up to $\pm$ 27°.

Classically, the process of geometric correction of images has been approached by employing two different methods (Billingsley, 1983), each of which requires knowledge of one or more ground control points (GCPs). The first one is based on orbital models, deliberately physical in conception, which aim to grasp and model the distortions in order to lead them back towards the desired cartographic projection. The second method, more empirical in conception, aims to convert the image into a map by finding transformation polynomials; this method usually requires a higher number of GCPs.

V. Palà is with the Institut Cartogràfic de Catalunya, Balmes 209-211, 08006 Barcelona, Catalonia, Spain.

X. Pons is with the Centre de Recerca Ecològica i Aplicacions Forestals (CREAF), and Unitat de Botànica, Fac. Ciències, Universitat Autònoma de Barcelona, 08193 Bellaterra, Catalonia, Spain.

In this study, we aim to

- incorporate the effect of relief into polynomial-based geometric correction models and apply them to TM (Landsat) and HRV (SPOT) images (the models have a different geometric fidelity, and they will be comparatively tested); and
- make an experimental check on the improvements achieved by these methods, comparing the results to those obtained using the classic polynomial models — in which account is not taken of relief — and to an orbital model (for SPOT only).

Orbital Models, Correction of SPOT Images, and Orbital Model Used

The ideal situation implementing a correction process based on physical models demands that the data be in a raw state, i.e., as captured at the sensor. In this situation, which we may consider equivalent to that of SPOT level 1A, the pixels have the nominal size (e.g., 10 m, 20 m, etc.) only at the nadir, while they are "bigger" the further we move to the sides of the image. In addition, other deformations must be taken into account, such as Earth curvature and rotation, orbital movement of the satellite, attitude of the sensor, non-linearity of sensor movement in the exploration devices (multispectral scanners), relief, etc.

Orbital models try to correct the image by taking into account the maximum number of these parameters and integrating them into a geocentric reference system (Labovitz and Marvin, 1986; Salamonowicz, 1986; Light, 1986; Marvin *et al.*, 1987; Gugan, 1987; Rodríguez *et al.*, 1988; Kratky, 1988). If we have a digital elevation model (DEM), we can correct for the effect of relief by means of the collinearity equations, that relate the position of each point of the territory (defined by its three Cartesian coordinates in the corresponding geometric space) with that of the sensor (also three coordinates). These equations require knowledge of the sensor attitude, defined by the three angles yaw (κ), roll (ω), and pitch (ϕ) (Wong, 1986). Various approaches can be taken in order to simplify the process, such as assuming that the attitude of the sensor is constant, or allowing that some parameter, such as pitch, changes linearly with time.

The main advantage of orbital models is their high precision and robustness, as a consequence of their physical foundations, while their chief disadvantages lie in their implementation complexity and, above all, the amount of calculation time required.

Although raw data correction by using orbital models may seem optimum, this is not the type of material that common users of high spatial resolution satellites usually re-

Photogrammetric Engineering & Remote Sensing, Vol. 61, No. 7, July 1995, pp. 935–944.

0099-1112/95/6107–935$3.00/0

quire. These users opt for Landsat TM or SPOT 1B products because they want the data for thematic studies — in which planimetric precision is not usually critical — rather than for pure cartography; those images are corrected for the major systematic distortions and are superimposed on a map by means of a simple polynomial correction. Furthermore, commercial software packages rarely offer the possibility of rectifying according to orbital models.

If there is no software available to apply orbital models, the 1A format images can be converted into 1B format using the coefficients provided by SPOT-Image. With regard to Landsat TM images, data in raw form are not usually commercialized, so that users cannot apply corrections based on orbital models; examples of this type of correction are to be found in Labovitz and Marvin (1986) and Marvin *et al.* (1987); this last work points out that orbital models for SPOT are easier to implement due to the absence of scanning machinery.

In order to verify the results of the different models we propose, we will use the Gugan (1987) orbital model on SPOT 1A images. That model has seven parameters: orbit semi-major axis, orbit inclination, true anomaly, ascending node, and three angles of sensor attitude. We have introduced two modifications into this model: the first consists in taking a constant orbital radius (circular orbit) on the set of rows of each image, and the second consists in allowing a change of attitude as a function of time. Attitude for SPOT images may be considered to be constant, or changes of all or some of the three angles may be allowed. Thus, for example, we find that Rodríguez *et al.* (1988) assume that the three angles are constant, while Salamonowicz (1986), Konecny *et al.* (1987), and Novak (1992) allow a linear change for all three angles, and Priebbenow and Clerici (1988) assume a linear variation for yaw and roll and a quadratic variation for pitch. We have decided to take yaw and roll as constant and allow a linear change in pitch as a function of time, so that there are four attitude parameters, and the model as a whole has eight parameters.

Models Based on Polynomials. Correction of Landsat TM and SPOT HRV Images

On a SPOT 1B image or on a Landsat TM image, the majority of the effects mentioned in the previous section (excepting relief) have been corrected by means of preprocessing. In the case of SPOT, this preprocessing is carried out using models based on third-degree polynomials, established to correct systematic deformations (conical perspective, curvature of the Earth, etc.) (SPOT-Image, 1986); in the case of TM, the effect of mirror movement and deviations of attitude (systematic correction; Labovitz and Marvin (1986)) are also corrected.

If the surface of the Earth had no mountains, these transformations would provide an image directly superimposable on a map using elementary transformations. These transformations (rotation, shift, and change of scale) are achieved by adjusting a first-degree polynomial with GCPs. This polynomial has the form

$$\mathbf{Col} = A + Bx + Cy \quad (1)$$
$$\mathbf{Row} = A' + B'x + C'y \quad (2)$$

in which

Col and **Row** are the column and row coordinates on the image,
x and y represent the map coordinates, and
A, B, C, A', B', C' are the polynomial coefficients.

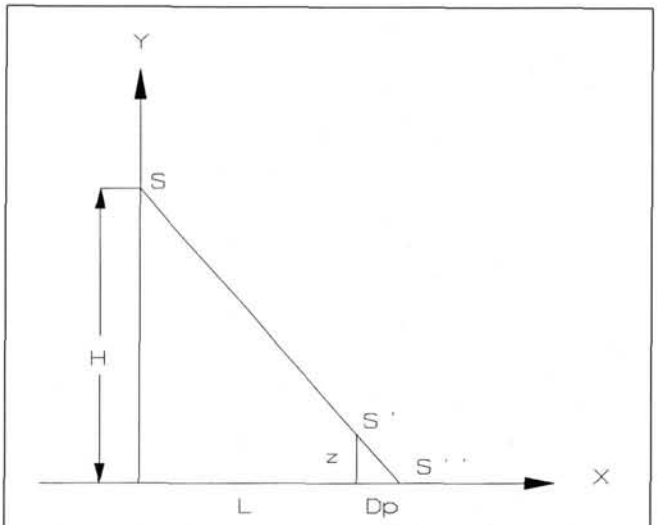

Figure 1. Displacement due to relief on a flat surface. Symbols defined in text.

Polynomial expressions are characterized by a great capability for absorption of accidental distortions. This is one of their most attractive aspects, as opposed to the rigidity of orbital models.

As noted earlier, these corrections do not include relief, so that, if the zone presents an uneven relief, it can be useful to apply a higher-degree polynomial in order to reduce deformation (Chuvieco, 1990). One should be reminded here that a higher-degree polynomial will almost always provide greater accuracy at the GCPs, although it will require more GCPs and will introduce unexpected effects far away from them, those effects being greater the higher the degree of the polynomial. The second-degree polynomials give the following expression:

$$\mathbf{Col} = A + Bx + Cy + Dx^2 + Ey^2 + Fxy \quad (3)$$
$$\mathbf{Row} = A' + B'y + C'y + D'x^2 + E'y^2 + F'xy \quad (4)$$

Billingsley (1983) shows the effects of each term of Equations 3 and 4.

Magnitude of the Displacement Due to Relief

It has sometimes been stated that the displacement due to relief is unimportant due to the enormous flight height of satellites in relation to the heights of mountains (Billingsley, 1983, page 763; Novak, 1992; Ardizone *et al.*, 1993). In other cases, the effect of relief is simply not mentioned (Lillesand and Kiefer, 1987), although, as we shall see below, that assumption is not entirely correct.

The effect of displacement due to relief depends very strongly on flight height, on the area taken in by each image (that is, the total field of view, or total FOV of the sensor), and, of course, on the magnitude of the relief. We will now formulate and quantify the amount of displacement, first without taking account of curvature of the Earth and then taking account of it.

Calculation of the Displacement without Taking Account of Curvature of the Earth

Presupposing a flat Earth, we must focus on the situation presented in Figure 1, in which the origin of coordinates is

TABLE 1. CALCULATION OF THE DISPLACEMENT DUE TO RELIEF CONSIDERING THE FLAT AND THE CURVED EARTH MODELS. EXAMPLE FOR LANDSAT-5 TM, AND FOR SPOT-1 HRV, GIVING H A VALUE OF 832 KM AND R A VALUE OF 6370 KM. INCLINATIONS ARE GIVEN FOR THE IMAGE MIDPOINT, AND THE CALCULATION IS DONE TAKING L CLOSE TO THE FURTHEST EDGE FROM THE SATELLITE NADIR. I: INCLINATION (SPOT, IMAGE CENTER); L: DISTANCE TO THE NADIR; z: POINT ELEVATION; DP: DISPLACEMENT DUE TO RELIEF.

	I	L	z	Dp (Flat Earth)	Dp (Curved Earth)	Difference
TM	—	90 km	3 km	384 m	427 m	43 m
				12.8 pixels	14.2 pixels	1.4 pixels
	—	90 km	1.5 km	192 m	213 m	21 m
				6.4 pixels	7.1 pixels	0.7 pixels
	—	50 km	3 km	214 m	237 m	24 m
				7.1 pixels	7.9 pixels	0.8 pixels
	—	50 km	1.5 km	107 m	118 m	12 m
				3.6 pixels	4.0 pixels	0.4 pixels
HRV	5.13°	106 km	3 km	385 m	435 m	50 m
				19.2 pixels XS	21.8 pixels XS	2.5 pixels XS
				38.5 pixels P	43.5 pixels P	5.6 pixels P
	5.13°	106 km	1.5 km	192 m	217 m	25 m
				9.6 pixels XS	10.9 pixels XS	1.3 pixels XS
				19.2 pixels P	21.7 pixels P	2.5 pixels P
	10°	179 km	3 km	648 m	735 m	87 m
				32.4 pixels XS	36.8 pixels XS	4.4 pixels XS
				64.8 pixels P	73.5 pixels P	8.7 pixels P
	10°	179 km	1.5 km	324 m	367 m	44 m
				16.2 pixels XS	18.4 pixels XS	2.2 pixels XS
				32.4 pixels P	36.7 pixels P	4.4 pixels P
	20°	339 km	3 km	1226 m	1402 m	177 m
				61.3 pixels XS	70.1 pixels XS	8.8 pixels XS
				122.6 pixels P	140.2 pixels P	17.7 pixels P
	20°	339 km	1.5 km	612 m	700 m	88 m
				30.6 pixels XS	35.0 pixels XS	4.4 pixels XS
				61.2 pixels P	70.0 pixels P	8.8 pixels P
	27°	464 km	3 km	1679 m	1942 m	262 m
				84.0 pixels XS	97.1 pixels XS	13.1 pixels XS
				167.9 pixels P	194.2 pixels P	26.2 pixels P
	27°	464 km	1.5 km	838 m	969 m	131 m
				41.9 pixels XS	48.4 pixels XS	6.5 pixels XS
				83.8 pixels P	96.9 pixels P	13.1 pixels P

the nadir of the sensor; the Y axis is defined by the line linking the sensor and the nadir; and the X axis, orthogonal to the former, links the point to be considered — at height 0 — with the origin of coordinates. We will call L the coordinate of this point along the X axis, z the height of this point, Dp the displacement in the direction of the X axis, H the flight altitude of the satellite over the reference surface, S the position of the satellite, S' the position of the problem point over the terrain, and S'' the projection of S' over the X axis.

At any given point, we have

$$H/z = (L + Dp) / Dp. \quad (5)$$

The displacement due to relief will be given by the equation

$$Dp = L{\cdot}z / [H - z]. \quad (6)$$

Given that H is much greater than z, the following simplification can be used for practical purposes:

$$Dp = L{\cdot}z/H \quad (7)$$

For Landsat, for example, and in very extreme cases — such as taking L = 90 km, z = 3 km, and H = 705.3 — this simplification involves an error of only 1.6 m (computed as the difference between Equations 6 and 7).

According to Equations 6 or 7, a lateral point of a TM image placed at 3,000 metres above sea level will be displaced by nearly 13 pixels. Nevertheless, it should be taken into account that the classic polynomial calculations (Equations 1 and 2) can scale the images and automatically spread the errors between the GCPs on the highest peaks and those on the deepest valleys or at sea level. Under such circumstances — for example, with heights between 0 and 3,000 metres in an image — we could have important errors of more than 6 pixels at sea level and at the peaks.

Calculation of the Displacement Taking Account of Curvature of the Earth

Appendix 1 provides a derivation of the displacement formula taking account of the curvature of the Earth. As can be observed, the calculation process is less direct than with the assumption of a flat Earth. Table 1 shows displacement values calculated using both methods, making clear that in extreme cases the differences can be substantial. As can be observed, consideration of Earth curvature is only of importance when we find major elevation differences at the edges of the image. For vertical SPOT images, the differences are smaller than in Landsat images, because the satellite flight height is 100 km higher and the field of view leaves 30 km on either side (some 2.5° per side). Similarly, in oblique views starting from 5.13°, the angle at the furthest lateral side edge from the nadir (at about 106 km or 7.28°) produces, for z = 3 km, displacements which are comparable to those of Landsat, although in pixels they are now considerably greater. Table 1 illustrates this effect, together with the fact that the curvature of the Earth becomes increasingly important with more oblique angles.

If we do not wish to allow displacements over a certain limit, we can calculate — for several distances L — which z would cause a displacement greater than that limit. Figure 2 shows these z values based on 2-km L intervals and at two limits: 0.5 pixels, which we consider to be the tolerable error limit in an *a priori* approach, and 0.2 pixels, which is that proposed by Marvin *et al.* (1987). For oblique SPOT views, this effect is even more significant.

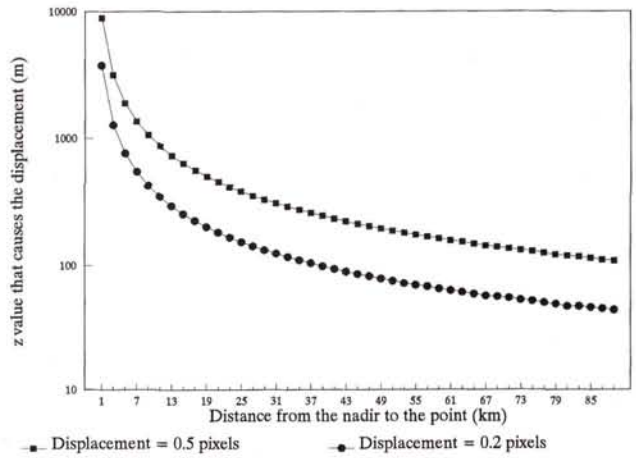

Figure 2. z Values that cause a displacement greater than 0.2 and 0.5 pixel, for points placed at different distances from the nadir. Calculations are done according to the curved Earth model and for a Landsat-5 TM image, taking R=6370 km and H=705.3 km. Ordinates in logarithmic scale.

Incorporation of Relief into the Models Based on Polynomials

As we mentioned earlier, the Landsat TM and SPOT 1B images have been "corrected" for the main distortions inherent in the geometry of the capturing system, so that, in order to adapt them to a certain cartographic projection, we have to apply first a transformation of the type rotation plus change of scale plus shift, and, then, correct for the effects of displacement due to relief. The first correction can be achieved with the aid of first-degree polynomials such as those described earlier; the second calls for consideration of the deformations produced by relief, and, as we have seen, at least two approximations are possible: one which takes account of the curvature of the Earth and one which does not.

In neither case is it essential to have an extremely detailed DEM, either planimetrically or altimetrically, because, as can be deduced from Equation 7, Z errors of 100 metres lead, for L = 90, to errors in displacement calculation lower than 0.5 pixels (Landsat).

In the next sections we outline several approximations which permit the incorporation of relief in models based on polynomials. Previously, it must be considered that

- We will be positing an inverse rectification model (Novak, 1992), in which image coordinates (Column, Row) will be obtained on the basis of the map coordinates (e.g., UTMx, UTMy).
- Once the coordinates (Column, Row) have been obtained, they must be repositioned taking account of displacement factors due to relief.
- In order to compute the displacement factors of the columns, we must know, for each row of the image, the column in which the nadir is situated. In the area covered by an image, the trajectory of the satellite can be considered as a straight line, and we will have a nadir equation with the form

$$\mathbf{Col} = m + n\cdot\mathbf{Row} \tag{8}$$

where **Row** is a row in the image, and **Col** is the column in which the nadir is situated in that row.
In the case of TM, and for a full frame, we could take the line which passes through the center of each row of the image. However, this would oblige us to consider, for each image, if we are working with a full frame, a quarter frame or a minor subscene, making the appropriate corrections in each case. Furthermore, for oblique SPOT images, it can prove even more difficult to decide which one is the straight line equation. We therefore felt that it would be more useful to leave m and n as unknowns, so that they could be deduced at each calculation.

In general terms, therefore, rectification of the columns will follow the next protocol: i.e.,

(1) For each pixel of the resulting image, whose map coordinates are known *a priori*, calculation is carried out using Equations 1 and 2 to find which coordinate ($\mathbf{Col}_1$, **Row**) in the original image would correspond (ignoring relief).
(2) Knowing **Row**, Equation 8 can be used to find the column in which the nadir is situated.
(3) The distance to the nadir column can now be calculated (parameter L).
(4) The height of that coordinate is read from the DEM and, using the appropriate formula (flat Earth or curved Earth models), the displacement undergone by that point is calculated (Dp).
(5) The column, $\mathbf{Col}_2$, on which the point of interest is projected is calculated and the DN corresponding to ($\mathbf{Col}_2$, **Row**) is read.
(6) If the rectification does not follow the nearest neighbor method, the necessary algorithms are applied (bilinear interpolation, etc.).

The rectification protocol of rows is almost the same, but modifying the third step to calculate the distance to the nadir row instead of the distance to the nadir column, and also changing the fifth step to obtain the row, $\mathbf{Row}_2$, in which the point is projected.

The parameters appearing in each approach can be obtained using the technique of unified approach to least-squares adjustement, described by Mikhail (1976) and used in a similar case by Salamonowicz (1986).

Incorporation of Relief in Calculating Columns

Model which Does not Take Account of Curvature of the Earth

The function to be minimized will be given by the next process, which follows the general protocol described above:

(1) $\mathbf{Row} = A' + B'x + C'y$
$\mathbf{Col}_1 = A + Bx + Cy$
(2) $\mathbf{Col}_n = m + n\cdot\mathbf{Row}$
(3) $L = \mathbf{Col}_1 - \mathbf{Col}_n$
(4) $Dp = L\cdot z/[H - z]$
(5) $\mathbf{Col}_2 = \mathbf{Col}_1 + Dp$

We should note that **Row** must be obtained in order to calculate the column of the nadir, $\mathbf{Col}_n$. If wished, the process can be summed up using the expression:

$$\begin{aligned}\mathbf{Row} &= A' + B'x + C'y \\ \mathbf{Col}_2 &= A+Bx+Cy \\ &\quad + \{\,[(A+Bx+Cy - \{m+n\cdot\mathbf{Row}\})\cdot z]/[H-z]\,\}\end{aligned} \tag{9}$$

Following this approach, there are five parameters (A, B, C, m, and n) to solve the expression of the columns. We will call this model the *flat Earth model.*

Simplification of the Previous Model. Integration into a Single Polynomial

Using the same simplification that allows us to derive Equation 7 from Equation 6, we can rewrite Equation 9 in the form

$$\mathbf{Col}_2 = A+Bx+Cy + \{ [(A+Bx+Cy - \{m+n\cdot\mathbf{Row}\})\cdot z]/H \} \quad (10)$$

We can substitute **Row** as a function of its expression (Equation 2) and, reordering terms, we have

$$\mathbf{Col}_2 = A + (B+B'n/H)x + (C+C'n/H)y + [(A/H) + (A'n/H) - (m/H)]z + (B/H)zx + (C/H)zy \quad (11)$$

We can now define the coefficients x, y, z, zx, and zy as new constants (B'', C'', D'', E'', and F'') and obtain directly the final expression of the columns: i.e.,

$$\mathbf{Col}_2 = A + B''x + C''y + D''z + E''zx + F''zy \quad (12)$$

Using this approach, there are six unknowns (A, B'', C'', D'', E'', F'') to solve the expression of the columns — one more than in the previous case — but this approach offers two advantages which make the expression attractive. First, it is not necessary to know the value of H, which adjusts automatically within the corresponding terms. Second, and in comparison with Equation 9, the polynomial obtained is easier to adjust to the GCPs and is faster to execute when rectifying the image.

On the other hand, we should note that the nadir line ($m + n\cdot\mathbf{Row}$) is not obtained explicitly, but is included within the general expression. The main advantage deriving from the dilution of the more physical parameters (H and the above-mentioned nadir line) is the greater flexibility of the model, which in some cases can absorb other non-systematic parameters which the strict flat Earth approach does not consider. However, this flexibility can represent a danger if the GCPs contain major location errors, because this problem will become less obvious in the adjustment process (though not in the test process).

Because Equation 12 is a polynomial, we will call the models which make use of it *polynomial models with z.*

Model Taking Account of the Curvature of the Earth

The function to be minimized will be given by the following process, which comes after the general process described above:

(1) $$\mathbf{Row} = A' + B'x + C'y$$
$$\mathbf{Col}_1 = A + Bx + Cy$$

(2) $$\mathbf{Col}_n = m + n\cdot\mathbf{Row}$$

(3) $$L = (\mathbf{Col}_1 - \mathbf{Col}_n)\cdot pix$$

Note that we must now multiply by pix in order to obtain L in the same magnitude as the map coordinates.

(4) The calculations of Appendix 1 are applied in order to find the displacement, Dp:

$$Dp = [(x_i - x_0)^2 + (y_i - y_0)^2]^{1/2}$$

(5) In the Dp calculation, its sign has been lost, so $\mathbf{Col}_2$ is calculated using the conditions:

if $L \geq 0$

$$\mathbf{Col}_2 = \mathbf{Col}_1 + Dp/pix \quad (13)$$

else

$$\mathbf{Col}_2 = \mathbf{Col}_1 - Dp/pix \quad (14)$$

Note that the **Row** must be obtained in order to calculate the nadir column, $\mathbf{Col}_n$.

In this approach there are five unknowns (A, B, C, m, and n) to resolve the expression of the columns, as in the case of the flat Earth model. It has the advantage of being physically more real than the two previous approaches, combined with the reliability of the more rigid models. On the other hand, as in the flat Earth models, it has the disadvantage of having to assume a value for H and of being even more complex to adjust and slower in calculation. We shall call this model the *curved Earth model.*

Incorporation of Relief in Obtaining Rows

Consideration of the effect of relief in the image rows is important if there is a certain pitch at the moment of capturing the image, or, in other words, if the sensor "looks forward or backward." The time required by SPOT HRV to take an image is about 9 seconds (Gugan, 1987), while that taken by Landsat TM is about 25 seconds (Labovitz and Marvin, 1986). If we call the angle of pitch ϕ, we can write

$$L = H\cdot\tan(\phi) \quad (15)$$

and rewrite Equation 6 as

$$Dp = H\cdot\tan(\phi)\cdot z/(H - z) \quad (16)$$

From this equation, it can be seen that a pitch value of 0.285° will lead to half-pixel deformations for z = 3 km when considering Landsat 5 TM. (It should be remembered that first-degree polynomials will tend to halve deformations, as they will spread them between the maximum and minimum measurements, as we mentioned above for columns.)

This effect is considered automatically in the orbital models, as they take account of the attitude of the sensor and allow for this possibility. In the case of SPOT, it is a recognized factor (Konecny *et al.*, 1987; Gugan, 1987; Priebbenow and Clerici, 1988; Kratky, 1988). In the case of Landsat, Beyer (1983) indicates the presence of movements with values in the range of $2\cdot10^{-4}$ degrees for Landsat 4 TM, and Labovitz and Marvin (1986) indicate values in the range of 10^{-6} degrees/second (1σ) for Landsats 4 and 5 after the systematic corrections; these quantities (certainly very small) seem to indicate that consideration of this effect on Landsat TM is not important. Nevertheless, we will test this experimentally.

Given that the angles of pitch are never very large and that the deformations arising in this case are potentially smaller than those which arise in the case of columns, we opted to ignore the curvature of the Earth. Assuming, therefore, a flat Earth, two approximations are possible: one considering the angle of pitch to be constant, and another which allows for an evolution of this angle throughout the rows of the image. In both cases we applied a model that is analogous to the polynomial with z because, for calculation of the displacement (Dp), it uses the simplification introduced into Equation 7.

Constant Pitch Model

In this case we will consider the distance to the nadir to be constant. The function to be minimized will be that given by the next process, which follows the general process de-

TABLE 2. PRINCIPAL CHARACTERISTICS OF THE IMAGES USED FOR THE EVALUATION OF THE DIFFERENT GEOMETRIC CORRECTION TECHNIQUES: ABBREVIATIONS TO REFER TO EACH OF THE IMAGES.

Abbrev.	Satellite/Sensor	Date/Orbital situation	Lateral inclination (SPOT)	Nr. of GCPs: Total Adjust./Test	zmin, zmax of GCPs (m): Total Adjust./Test
TM	Landsat-5/ TM	13-Jul-90/ 198-031	—	38 25/13	7,1746 7,1746/73,1740
SP_P	SPOT-1/ HRV-Pancrom.	3-Jul-89/ 043-265	9.7°	31 20/11	290,2020 480,1940/290,2020
SP_XS	SPOT-1/ HRV-Multisp.	25-Jul-91 042-265	10.4°	25 17/8	475,1920 475,1920/400,1730
SEG_P	SPOT-1/ HRV-Pancrom.	5-Set-88/ 045-264 045-265 045-266 045-267	2.3°	31 20/11	2,1610 2,1610/90,1560

scribed above:

(1) $\mathbf{Row}_1 = A' + B'x + C'y$
(2) (not necessary)
(3) L is a constant
(4) $Dp = L{\cdot}z/H$
(5) $\mathbf{Row}_2 = \mathbf{Row}_1 + Dp$

$\mathbf{Row}_1$ and $\mathbf{Row}_2$ are, respectively, the row in which we would read whether there was any displacement due to relief and the row on which it has been projected.

The process can be summarized by the expression

$$\mathbf{Row}_2 = A' + B'x + C'y + L{\cdot}z/H \quad (17)$$

which, by defining a new unknown, D''', as $L{\cdot}z/H$, can be rewritten in simple polynomial form as

$$\mathbf{Row}_2 = A' + B'x + C'y + D'''z. \quad (18)$$

In this approach, there are four unknowns (A', B', C', D''') to solve the expression of the rows. We shall call this model the *constant pitch model.*

Model of Variable Pitch throughout the Rows

In this case, we will allow for a change in the pitch angle throughout the rows of the image; this change is presumed to be a linear function of the **Row** parameter. The distance to the nadir (L) will, therefore, no longer be constant, and should be defined in the following form:

$$L = g{\cdot}\mathbf{Row} + h. \quad (19)$$

The function to be adjusted will be given by the following process, which comes after the general process described above: i.e.,

(1) $\mathbf{Row}_1 = A' + B'x + C'y$
(2) (not necessary)
(3) $L = g{\cdot}\mathbf{Row}_1 + h$
(4) $Dp = L{\cdot}z/H$
(5) $\mathbf{Row}_2 = \mathbf{Row}_1 + Dp$

The process can be summarized by the expression

$$\mathbf{Row}_2 = A' + B'x + C'y + [g{\cdot}(A' + B'x + C'y) + h]{\cdot}z/H. \quad (20)$$

Reordering terms and defining new coefficients (D''', E''', F'''), we obtain once more a polynomial form for the rows: i.e.,

$$\mathbf{Row}_2 = A' + B'x + C' + D'''z + E'''zx + F'''zy \quad (21)$$

With this approach, there are six unknowns (A', B', C', D''', E''', F''') to resolve the expression of the rows. We shall call this model the *variable pitch model.*

Images, Data, and Evaluation Methods

Images and Data Used

In order to compare the results obtained with the different techniques outlined, we used GCPs on TM and SPOT images over the central and eastern Pyrenees, in areas of strong hypsometric contrasts. The points were sought on the 1:5,000-scale (UTM projection) orthophotomaps published by the Institut Cartogràfic de Catalunya (ICC). The elevations (z) of the GCPs were obtained from the DEM of the ICC (resolution in x and y: 15 m).

Table 2 provides a summary of the principal characteristics of these images, together with the abbreviations which we will use henceforth.

Evaluation Methods

For each geometrical correction method proposed, we evaluated its precision, its simplicity of implementation, and its performance.

In order to evaluate precision, we applied the most frequently used estimator in geometrical corrections, i.e., the square root of the mean of the residual error squared at each GCP, which, following Slama (1986), we will simply call RMS. We shall define RMS_c as the error in estimation of the columns, RMS_r as the error in determination of rows, and RMS as the error in the overall determination of columns and rows.

GCPs are not always available at the extreme parts of the image in columns and elevation, so we have usually neither adjusted nor test points subjected to the maximum deformations. Nevertheless, if a model seems to behave clearly worse in the test than in the adjustment, it is feasible to think that it will still show more aberrant behavior in the most critical zones of the image.

Finally, and in order to analyze the performance, we proceeded to rectify a 1024- by 1024-pixel SPOT frame, using a single computer (VAXStation 3100) and taking a DEM of 30 m between points.

Results and Discussion

We will use the following notation:

P1 refers to a first-degree polynomial correction;
P2 refers to a second-degree polynomial correction;
PZ IN C refers to a first-degree polynomial correction for the columns according to the *polynomial model with z*;
FE IN C refers to a first-degree polynomial correction for the columns with correction of displacement due to relief according to the *flat Earth model*;
CE IN C refers to a first-degree polynomial correction for the columns with correction of displacement due to relief according to the *curved Earth model*;
PZ1 IN R refers to a first-degree polynomial correction for the rows, which integrates the z values according to the *constant pitch model*;
PZ2 IN R refers to a first-degree polynomial correction for the rows, which integrates the z values according to the *variable pitch model*; and
ORBITAL refers to the orbital correction outlined in the corresponding section, which simultaneously determines rows and columns.

Columns

Table 3 shows the RMS errors produced by the different methods of geometric correction in obtaining the columns, for both adjustments and tests.

TM: We can clearly highlight two facts. First we can see that, with respect to the classic polynomial corrections, the introduction of relief provides an improvement both in the adjustments and in the tests. The most notable difference concerns the first-degree polynomial, which does not manage to reduce the error below a pixel. With respect to the second-degree polynomial, we see that, although it does give better results than the first-degree polynomial, the errors remain higher than any of the models with z. The second fact to be emphasized is that the three models with z provide very similar results, any of them appearing to be clearly better than the others.
SP_P: We see that the strong lateral inclination makes it impossible to achieve satisfactory correction with first- or second-degree polynomials; we should note that, in an area in which the GCPs are distributed along an elevation interval of nearly 2,000 metres, the errors are very large, never falling below an average of 5.5 pixels, which means that the errors at higher or lower elevations are even greater. The improvement obtained with the incorporation of relief is radical: the error level is well below one pixel, being highly similar to that achieved with the orbital model. As in the case of TM, the three models with z give comparable results.
SP_XS: The situation here is similar to the previous case, although the errors are smaller. We might note, too, that the second-degree polynomial gives misleading error values in the adjustment, because nearly all of them are doubled in the test; this foreseeable fact has already been mentioned above.
SEG_P: The more moderate lateral field of view (2.3°) means that the response of the polynomials is not as defective as before, though it remains unsatisfactory, especially on the test points. Once again, the results with incorporation of relief into the polynomial-based models are highly satisfactory, giving even subpixel precision in this segment of four SPOT P images. Despite the results not seeming to be as good as in the orbital model, it is remarkable that such simple models as **PZ** can maintain high geometrical quality throughout 200 by 60 kilometres of image with pixels of 10 m. We think this can be explained by the model's ability to absorb the different variables which contribute in the image geometry.

In short, regarding the different geometrical correction models for obtaining the columns, the orbital model appears to be highly solid, because it retains very low error levels in all situations. Protocols which incorporate relief into polynomial-type models also provided very acceptable results for cartographic applications in all the situations considered, even in the case of segments of four SPOT images. Among the various models tested, the curved Earth model always came out the best or amid the best results; outstanding for its simplicity and good results is the model which integrates the elevations into a single polynomial (**PZ**). The results in models which incorporate altitudes were always better than those obtained with the classic polynomials, although some of the models we posited had a degree of complexity very similar to the latter and much lower than that of the orbital models.

Rows

Table 3 shows the RMS errors produced by the different geometrical correction methods in obtaining rows.

TM: There seems to be a distortion factor which is not explained by the first-degree polynomial or by the constant pitch model, in view of the small improvement obtained by using a second-degree polynomial or, even more so, the variable pitch model. The results are nevertheless acceptable in all cases, which is in accordance with the absence of major pitch in the TM data about which we commented earlier.
SP_P: We see that the more mathematically complex polynomial-based models (**P2** and **PZ2**) present worse results in the test. Probably the real pitch of the satellite was small and, in this case, these models only explain accidental variations or imprecisions in the placing of the GCPs, which means that the adjusted function does not respond optimally with the test points.
SP_XS: The pitch consideration does seem to be important here, and we thus achieve results which are perfectly comparable with the orbital model (**PZ1**) or even better (**PZ2**). On the other hand, despite the good results in the adjustment, the second-degree polynomial is unable to provide satisfactory test results.
SEG_P: The results point again to the advisability of considering a variable pitch throughout the image, as in the orbital model or in **PZ2**, although the second-degree polynomial also gives good results.

In short, regarding the different geometrical correction methods for obtaining rows, we can conclude that the orbital model proves once more to be the most suitable one, although in the majority of cases the variable pitch consideration integrated into the rows polynomial can provide very acceptable results. We should nevertheless point out that in this case the errors detected are much smaller and consideration of relief is not so necessary.

Columns and Rows Together

Table 3 shows the overall RMS errors produced by the different geometrical correction methods for obtaining the columns and rows together; we will not provide details here, however, because the appropriate argument can be deduced by combining the remarks made for columns and rows separately.

Note: In all these cases, when the treatment for rows is not specified, it should be understood that a first-degree polynomial was applied.

Performance

Table 4 shows the time taken by a VAXStation 3100 computer to correct an image of 1024 pixels by 1024 pixels with the methods posited; we have also indicated there the execution factor time with respect to **P1**. In view of the results, we can classify the processes into three groups:

The first is made up of those methods which involve a

TABLE 3. RMS ERROR (IN PIXELS) PRODUCED BY THE DIFFERENT METHODS IN OBTAINING THE COLUMNS, THE ROWS, AND COLUMNS AND ROWS TOGETHER. NOTATION IN TEXT.

COLUMNS

Method:		P1	P2	PZ IN C	FE IN C	CE IN C	ORBITAL
TM	Adjust.	1.41	0.75	0.70	0.70	0.70	—
	Test	1.07	0.62	0.56	0.57	0.53	—
SP _ P	Adjust.	6.41	5.51	0.59	0.60	0.59	0.61
	Test	6.83	5.73	0.68	0.72	0.68	0.59
SP _ XS	Adjust.	2.09	1.76	0.68	0.71	0.72	0.60
	Test	2.43	3.29	0.92	0.86	0.85	0.67
SEG _ P	Adjust.	1.20	1.08	0.66	0.66	0.67	0.50
	Test	1.87	1.52	0.75	0.74	0.73	0.52

ROWS

Method:		P1	P2	PZ1 IN F	PZ2 IN F	ORBITAL
TM	Adjust.	0.60	0.51	0.59	0.47	—
	Test	0.77	0.69	0.79	0.64	—
SP _ P	Adjust.	0.56	0.38	0.55	0.55	0.55
	Test	0.60	0.76	0.60	0.69	0.57
SP _ XS	Adjust.	0.80	0.73	0.58	0.52	0.58
	Test	1.05	1.08	0.73	0.54	0.72
SEG _ P	Adjust.	0.52	0.41	0.51	0.47	0.49
	Test	0.73	0.56	0.73	0.65	0.47

COLUMNS AND ROWS

Method:		P1	P2	PZ IN C	PZ IN C + PZ1 IN R	PZ IN C + PZ2 IN R	FE IN C	CE IN C	CE IN C + PZ1 IN R	CE IN C + PZ2 IN R	ORBITAL
TM	Adjust.	1.53	0.90	0.92	0.92	0.84	0.92	0.92	0.92	0.84	—
	Test	1.32	0.93	0.95	0.97	0.85	0.96	0.93	0.95	0.83	—
SP _ P	Adjust.	6.44	5.53	0.81	0.81	0.81	0.82	0.81	0.81	0.81	0.82
	Test	6.86	5.78	0.91	0.90	0.97	0.93	0.90	0.90	0.96	0.82
SP _ XS	Adjust.	2.23	1.90	1.05	0.89	0.86	1.07	1.08	0.93	0.89	0.83
	Test	2.65	3.47	1.40	1.18	1.07	1.36	1.35	1.12	1.00	0.98
SEG _P	Adjust.	1.30	1.16	0.84	0.83	0.81	0.84	0.84	0.84	0.82	0.70
	Test	2.01	1.68	1.03	1.04	0.99	1.03	1.02	1.03	0.97	0.70

moderate increase factor (of 1.06× to 1.24×) of rectification time. This is the case of the second-degree polynomial (which, not using DEM, becomes the fastest), of the flat Earth, and of the integrated polynomial methods.

The second group is made up of all the processes in which the curved Earth model intervenes, whose much greater calculation complexity practically doubles rectification time.

In these two groups, the method used in correction of the rows (**P1**, **PZ1**, or **PZ2**) involves very small increases in execution time.

The third group contains the orbital model, which proves to be extraordinarily slower, due to the enormous volume of calculation involved in it.

We should state, finally, that analysis of these data must be undertaken bearing in mind that, in writing the necessary rectification programs, the goal pursued was not optimization, but rather ensuring that the processes were as closely comparable as possible.

Conclusions

The improvement achieved by introducing relief into the corrections is numerically evident and methodologically notable. With a simple and easily implemented approach, we have achieved subpixel errors in columns and rows in all the tests carried out, even in the case of SPOT images with quite large lateral fields of view (10.4°) or in segments of four panchromatic images.

We could summarize the main characteristics of the proposed models as follows:

Simplicity:
- The implementation of the necessary programs (adjustment on the basis of GCPs and rectification of images) is simple.
- The models are well-behaved outside the GCPs.

TABLE 4. PROCESSING TIME TO CORRECT A 1024- BY 1024-PIXEL IMAGE AND FACTOR WITH RESPECT TO P1. NOTATION IN TEXT.

P1	P2	PZ IN C	PZ IN C + PZ1 IN R	PZ IN C + PZ2 IN R	FE IN C	CE IN C	CE IN C + PZ1 IN R	CE IN C + PZ2 IN R	ORBITAL
1'25"	1'33"	1'38"	1'52"	1'55"	1'42"	2'44"	2'45"	2'53"	35'24"
×1.00	×1.06	×1.10	×1.22	×1.24	×1.14	×1.95	×1.96	×2.02	×28.19

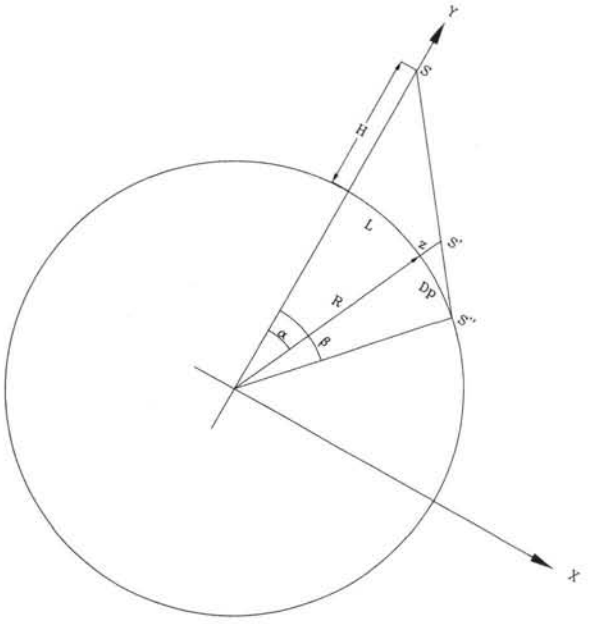

Figure A1. Displacement due to relief on a curved surface. Symbols defined in text.

Fidelity: • The models provide good accuracy; for both adjustments and tests we obtain subpixel RMS errors even for oblique SPOT images. The results are better than those obtained with the classic polynomial methods, and, for SPOT, almost as good as those obtained with orbital models.

Performance: • Rectification takes place almost as quickly as with the classic polynomial models.

These characteristics lead us to suggest the application of these models in rectification of Landsat and SPOT images, with the following considerations:

Landsat: Although the improvement is not extremely important with respect to a second-degree polynomial, the mere fact of this gain and the more physical basis of the models with z make consideration of relief for obtaining columns advisable. We might further indicate that, if we had had GCPs on the highest peaks of the Pyrenees and in the deepest valleys, then the improvement noted would probably have been even greater.

SPOT: We found that the orbital model represented the most solid correction alternative, although it turns out to be much slower; if an orbital model is not available or if calculation time is a limitation, then the models posited represent an excellent solution, the more necessary the more oblique the image is.

With respect to the rows, it would seem that consideration of variable pitches provides slight improvements for both Landsat and SPOT, though it must be borne in mind that this requires the determination of six unknowns, compared to the three necessary in a first-degree polynomial.

For obtaining columns, the adoption of one of the three models which incorporate hypsometry into the polynomials will depend on our interests and calculation capacity; we nevertheless believe that the flat Earth model does not offer any special advantage and that the real difference arises between the polynomial model with z (very simple implementation, six unknowns, fast execution, and high reliability) and the curved Earth model (much more complex implementation, five unknowns, slower execution, and apparently better results). We decided to choose the polynomial model with z, because the improvements which the curved Earth model seemed to provide in some cases were small in comparison with the advantages of the polynomial model with z. We should nevertheless stress the need for carrying out tests when tackling models such as this one, very flexible due to the absence of explicit physical parameters. If a sufficient number of points is not available to carry out tests, work with the curved Earth model may be more reliable; besides, this model has one fewer unknown.

We should note, finally, that the incorporation of elevation values into geometric correction models has implications in the selection of GCPs, because the placing of points at very extreme levels (maxima and minima) not only does not distort the model but also proves to be a major factor for optimum adjustment.

Appendix

Derivation of the Displacement Assuming an Spherical Earth

To facilitate the calculation, we assume that the Earth radius is constant. This is a feasible approximation because, for SPOT HVR or Landsat TM images, the Earth radius variations are insignificant. An average radius can be calculated based on latitude with the following equation:

$$R = [b^2+\cos^2(\text{Lat})\cdot(a^2-b^2)]^{1/2} \quad \text{(A1)}$$

where a and b are the major and minor Earth axes, and Lat is the latitude at the center of the image to be rectified.

A flat, Cartesian, and geocentric reference system is established, with the Y axis defined by a line linking the satellite with the Earth center, and the X axis crossing the Earth center orthogonally.

Following Figure A1, we name H the flight height of the satellite over the area of reference; S the position of the satellite; S' the position over terrain of the point to be considered; S'' the point at which S' is projected; z the elevation of this point; L the distance from the point to the nadir measured along the Earth surface from the sensor nadir on each row; and Dp the displacement due to relief, which we want to evaluate.

The displacement value (Dp) at a point due to the combined effect of relief and Earth curvature results in an arc defined by the angle ($\alpha - \beta$) on Figure A1. The angle α is known from the distance L on the Earth surface: i.e.,

$$\alpha = L/R \quad \text{(A2)}$$

The line equation that links the sensor (S) and the point on the terrain (S'') is

$$y = ex + f \quad \text{(A3)}$$

where

$$e = \{[R+z]\cdot\cos(\alpha)-[R+H]\}/\{[R+z]\cdot\sin(\alpha)\} \quad \text{(A4)}$$

$$f = R + H \quad \text{(A5)}$$

Now we should calculate the intersection of this line with the the Earth circumference, but this is slow to calcu-

late and does not offer a unique solution. For this reason, it is convenient to assume the arc *Dp*, because of its tiny dimension, as a rectilinear segment (an example of linear introduction to optimize processes in orbital models can be found in Marvin *et al.* (1987)). We can say that this line is defined by the equation

$$y = cx + d \quad \text{(A6)}$$

Letting (X_0, Y_0) to be the base coordinates of the point S' on the reference surface level, defined by the expressions

$$x_0 = R \cdot \sin(\alpha) \quad \text{(A7)}$$

$$y_0 = R \cdot \cos(\alpha) \quad \text{(A8)}$$

We can now deduce the coefficients c and d

$$c = -\tan(\alpha) \quad \text{(A9)}$$

$$d = y_0 - c \cdot x_0 \quad \text{(A10)}$$

The coordinates (x_i, y_i) of S'', corresponding to the intersection between the two lines, can be calculated with the expressions

$$ex + f = cx + d \quad \text{(A11)}$$

$$x_i = (d - f)/(e - c) \quad \text{(A12)}$$

$$y_i = e \cdot x_i + f \quad \text{(A13)}$$

The displacement value can be finally calculated with

$$Dp = [(x_i - x_0)^2 + (y_i - y_0)^2]^{1/2} \quad \text{(A14)}$$

References

Ardizone, J., A. Arozarena, J. Delgado, M. Herrero, G. Villa, and P. Vivas, 1993. Análisis estadístico para la corrección geométrica de imágenes de satélite, *Proceedings of the IV Reunión Científica de la Asociación Española de Teledetección*, Sevilla, Spain, November 1991, pp. 78-85.

Beyer, E.P., 1983. Thematic Mapper Geometric Correction Processing, *Seventeenth International Symposium on Remote Sensing of the Environment*, Ann Arbor, Michigan, pp. 319-334.

Billingsley, F.C., 1983. Data Processing and Reprocessing, *Manual of Remote Sensing* (R.N. Colwell, editor), American Society of Photogrammetry, Falls Church, Virginia, pp. 719-792.

Chuvieco, E., 1990. *Fundamentos de teledetección espacial*, Rialp, Madrid, Spain, 453 p.

Gugan, D.J., 1987. Practical Aspects of Topographic Mapping from SPOT Imagery, *Photogrammetric Record*, 12(69):349-355.

Kratky, V., 1988. Rigorous Stereophotogrammetric Treatment of SPOT Images, *Colloque International SPOT-1: Utilisation des images, bilan, résultats*, Paris, France, pp. 1281-1288.

Konecny, G., P. Lohmann, H. Engel, and E. Kruck, 1987. Evaluation of SPOT Imagery on Analytical Photogrammetric Instruments, *Photogrammetric Engineering & Remote Sensing*, 53(9):1223-1230.

Labovitz, M.L., and J.W. Marvin, 1986. Precision in Geodetic Correction of TM Data as a Function of the Number, Spatial Distribution, and Success in Matching of Control Points: A Simulation, *Remote Sensing of the Environment*, 20:237-252.

Light, D.L., 1986. Satellite Photogrammetry, *Manual of Photogrammetry* (C.C Slama, editor), American Society of Photogrammetry, Falls Church, Virginia, pp. 883-977.

Lillesand, T.M., and R.W. Kiefer, 1987. *Remote Sensing and Image Interpretation*, John Wiley & Sons, New York, N.Y., 721 p.

Marvin, J.W., M.L. Labovitz, and R.E. Wolfe, 1987. Derivation of a Fast Algorithm to Account for Distortions Due to Terrain in Earth-Viewing Satellite Sensor Images, *IEEE Transactions on Geoscience and Remote Sensing*, GE-25 (2):244-251.

Mikhail, E.M., 1976. *Observations and Least Squares*, IEP, New York, N.Y.

Novak, K., 1992. Rectification of Digital Imagery, *Photogrammetric Engineering & Remote Sensing*, 58(3):339-344.

Priebbenow, R., and E. Clerici, 1988. Cartographic Applications of SPOT Imagery, *Colloque International SPOT-1: Utilisation des images, bilan, résultats*, Paris, France, pp. 1189-1194.

Rodríguez, V., P. Gigord, A.C. de Gaujac, and P. Munier, 1988. Evaluation of the Stereoscopic Accuracy of the SPOT Satellite, *Photogrammetric Engineering & Remote Sensing*, 54(2):217-221.

Salamonowicz, P.H., 1986. Satellite Observation and Position for Geometric Correction of Scanner Imagery, *Photogrammetric Engineering & Remote Sensing*, 52(4):491-499.

Slama, C.C (editor), 1986. *Manual of Photogrammetry*, American Society of Photogrammetry, Falls Church, Virginia, 1056 p.

SPOT-Image, 1986. *SPOT Standard CCT Format*, SPOT-Image, Toulouse, pp. 13.4-13.5.

Wong, K.W., 1986. Basic Mathematics of Photogrammetry, *Manual of Photogrammetry* (C.C Slama, editor), American Society of Photogrammetry, Falls Church, Virginia, pp. 37-101.

(Received 1 April 1993; accepted 21 October 1993)

Vicenç Palà

Vicenç Palà received his B.Eng. in Computer Science from the Universitat Politècnica de Catalunya (UPC) in 1984. From 1982 to 1986 he was researcher at the UPC Computing Center, developing digital processing tools in the Remote Sensing domain. Since 1987 he has been working as Head of Image Processing and Systems Development at the Institut Cartogràfic de Catalunya, where he is currently involved in projects related to image processing, geocoding, and animation.

Xavier Pons

Xavier Pons received his B.S. in Biology in 1988, the M.S. in Botany in 1990, and the Ph.D. in Remote Sensing and G.I.S. in 1992, all from the Universitat Autònoma de Barcelona. His main work has been done in radiometric and geometric corrections of satellite imagery, in cartography of ecological and forestry parameters from airborne sensors, and in studies of the spectral response of Mediterranean vegetation. He is currently working in descriptive climatology models and modeling forest fire dynamics and hazards.